Resonance recombination model and quark distribution functions in the quark-gluon plasma

L. Ravagli, H. van Hees,[*] and R. Rapp

Cyclotron Institute and Physics Department, Texas A&M University, College Station, Texas 77843-3366, USA

(Received 17 June 2008; revised manuscript received 19 March 2009; published 12 June 2009)

We investigate the consequences of space-momentum correlations in quark phase-space distributions for coalescence processes at the hadronization transition. Thus far it has been proved difficult to reconcile such correlations with the empirically observed constituent quark number scaling (CQNS) at the Relativistic Heavy Ion Collider (RHIC). To address this problem we combine our earlier developed quark recombination model with quark phase-space distributions computed from relativistic Langevin simulations in an expanding quark-gluon plasma (QGP). Hadronization is based on resonance formation within a Boltzmann equation that recovers thermal equilibrium and obeys energy conservation in the quark-coalescence process, while the fireball background is adjusted to hydrodynamic simulations of semicentral Au-Au collisions at RHIC. To facilitate the applicability of the Langevin process, we focus on strange and charm quarks. Their interactions in the QGP are modeled using leading-order perturbative QCD augmented by effective Lagrangians with resonances that smoothly merge into hadronic states formed at T_c. The interaction strength is adjusted to reproduce the empirical saturation value for the quark-elliptic flow, $v_{2,q}^{\text{sat}} \simeq 7$–$8\%$. The resulting ϕ and J/ψ elliptic flow recover CQNS over a large range in transverse momentum (p_T) within a few percent. As a function of transverse kinetic energy, both the quark spectra from the Langevin simulations and the meson spectra generated via resonance recombination recover CQNS from zero to at least 3 GeV.

I. INTRODUCTION

The mechanism of hadronization, i.e., the conversion of quarks and gluons produced in hadronic or electromagnetic reactions into colorless hadrons, is a nonperturbative problem that is presently not calculable within the theory of strong interactions, quantum chromodynamics (QCD). For partons produced at large transverse momentum, p_t, the factorization theorem of QCD allows to treat the hadronization process via a so-called fragmentation function, which is universal and can, in principle, be determined empirically. At low momentum this scheme is no longer applicable and other hadronization mechanisms become relevant. The quark coalescence model (QCM) has provided a phenomenologically successful framework to understand several nonperturbative features of hadron production in hadronic collisions. In elementary (p-N and π-N) reactions, flavor asymmetries in kaon and charmed hadron spectra have been associated with the recombination of produced strange and charm quarks with valence (and sea) quarks in target and projectile [1–3]. In heavy-ion reactions at the Super Proton Synchrotron (SPS) [4] and the Relativistic Heavy Ion Collider (RHIC), recombination of quarks from a thermalized quark-gluon plasma (QGP) [5–14] gives a simple and intuitive explanation of several unexpected features in the observed hadron spectra, most notably the large baryon-to-meson ratio and the rather universal constituent quark number scaling (CQNS) of the elliptic flow coefficient, $v_{2,h}(p_T) \equiv n_q v_{2,q}(p_T/n_q)$ (n_q: number of valence quarks in hadron h;

p_T: transverse momentum of h). This scaling relation implies the momenta of the coalescing quarks to be collinear, and its implementation in QCMs usually restricts their applicability to sufficiently large momenta so that the associated nonconservation of energy in the hadron formation process is small. Since at high p_T parton fragmentation is expected to take over, the typical range of applicability of QCMs is at intermediate momenta, $2 \text{ GeV} \lesssim p_T \lesssim 6 \text{ GeV}$. In our recent work [12], we have suggested a reinterpretation of quark coalescence in terms of hadronic resonance formation, implemented via $q + \bar{q} \to M$ scattering into a Boltzmann equation (M: meson). Energy conservation is obeyed by utilizing hadronic reaction rates, along with detailed balance, based on pertinent spectral functions. In addition, we have shown that this approach correctly recovers the thermal equilibrium limit, which enabled a more controlled extension of the coalescence mechanism to low p_T and to make contact with the phenomenologically successful hydrodynamic description of bulk matter at RHIC.

Another aspect that has evaded a satisfactory explanation in QCMs at RHIC is the question of space-momentum correlations in the underlying (thermal) quark distribution functions (see, e.g., Ref. [15] for a recent critical review). In hydrodynamic models the elliptic flow of produced hadrons is a collective effect that implies a definite correlation between the particle's momentum and its spatial position in the fireball, i.e., a (locally thermalized) fluid cell moving into a specific direction preferentially emits hadrons in that same direction. Such a correlation is neglected within the so-called factorized implementation of the parton $v_{2,q}(p_T)$ that does not carry any spatial dependence (and is therefore identical regardless of the quark's position inside the fireball). While this approximation straightforwardly recovers the empirical constituent-quark number scaling (CQNS) of the hadron elliptic flow, it is

———

[*]Present address: Institut für Theoretische Physik, Justus-Liebig-Universität Giessen, Heinrich-Buff-Ring 16, D-35392 Giessen, Germany.

at variance with the hydrodynamic description of v_2 as a collective expansion effect.

Previous attempts to incorporate space-momentum correlations into QCMs have found the empirically observed CQNS to be rather fragile [16–18]. Part of the problem is the construction of a realistic transition from the thermal to the kinetic regime of the underlying parton phase-space distribution functions, as characterized by the "saturation" (leveling off) of the empirical parton v_2 at about $p_t \simeq 1$ GeV. In Ref. [16] several elliptic "deformations" of a thermal blast-wave parametrization have been considered, motivated by different plausible realizations of v_2. While some features could be ruled out being incompatible with the empirical CQNS, other assumptions did not spoil the latter. In Ref. [18] a reduction of the boost velocity at higher momenta was introduced, entailing a violation of CQNS at the 20% level. It therefore seems that purely phenomenological prescriptions of space-momentum correlations and associated v_2 did not arrive at a conclusive interpretation of the key features underlying the quark distribution functions. In Ref. [17], based on numerical transport simulations, it was even argued that rather delicate cancellations must be at work to obtain CQNS for the thermal components, thus raising doubts on the robustness of the coalescence approach. In view of the broad empirical applicability of CQNS across different centralities, system sizes, and collision energies [19,20], such an interpretation would be difficult to reconcile with experiment.

In the present article we adopt a microscopic approach to compute quark distributions in four-dimensional phase space (transverse position and momentum) by employing relativistic Langevin simulations for strange and charm quarks within an expanding thermal QGP background. In a strict sense, the underlying Fokker-Planck equation is applicable for a diffusive treatment of heavy and/or high-momentum quarks, i.e., in a regime where the momentum transfers from the heat bath are small. Our simulations for low-momentum ($p_t \lesssim 1$ GeV) strange quarks are thus at the boundary of applicability of a Fokker-Planck treatment and may be considered as extrapolations thereof. The Langevin approach has the attractive feature that it naturally encodes the transition from a thermal to a kinetic regime. In particular, when simulating heavy-quark (HQ) motion in an expanding QGP fireball for noncentral collisions, this transition reflects itself in a saturation of the elliptic flow [21,22], a key ingredient to CQNS in light-hadron spectra observed at RHIC. It turns out that Langevin simulations preserve the v_2 saturation feature when applied to strange quarks (with thermal masses of ∼0.5 GeV). We will therefore investigate whether the resulting quark distribution functions, evolved to the hadronization transition and injected into our resonance recombination approach, allow for a better (microscopic) understanding of space-momentum correlations in the coalescence process. In view of the rather delicate dependence of CQNS on these correlations (as discussed above), a realistic treatment of the kinematics in the hadron formation process is mandatory, including energy-momentum conservation, noncollinear kinematics, and a well-defined equilibrium limit. The recombination approach developed in Ref. [12] satisfies these requirements. In addition to this, the QGP evolution and subsequent hadronization are linked via

the ansatz that resonances play an essential role in hot QCD matter around T_c. This scenario is consistent with effective potential models where a nonperturbative description of the strongly coupled QGP (sQGP) is realized via bound [23] and/or resonance [24,25] states of deconfined partons. Recent lattice QCD computations support the picture of various (light and strange) hadronic states surviving up to temperatures of ∼1.5–2T_c [26,27].

Our article is organized as follows. In Sec. II we review our earlier developed model [12] for resonance hadronization based on the Boltzmann equation. In Sec. III we elaborate the computation of the phase-space distributions of quarks obtained from Langevin simulations of an expanding QGP fireball at RHIC. In Sec. IV we discuss the numerical results for the v_2 coefficients of ϕ and J/ψ mesons within our model, and discuss their properties in terms of CQNS in both transverse momentum and transverse kinetic energy, K_T. Section V contains our conclusions.

II. RECOMBINATION FROM THE BOLTZMANN EQUATION

Following Ref. [12], our description of hadronization at the critical temperature, T_c, is based on the Boltzmann equation using resonance quark-antiquark cross sections to compute meson spectra in terms of underlying anti-/quark phase-space distributions, $f_{q,\bar{q}}$ (baryons could be treated in a similar way, e.g., in a two-step process using subsequent quark-quark and quark-diquark interactions; in the present article, we will focus on mesons). The meson phase-space distribution, F_M, is determined by the equation

$$\left(\frac{\partial}{\partial t} + \boldsymbol{v} \cdot \boldsymbol{\nabla}\right) F_M(t, \boldsymbol{x}, \boldsymbol{p}) = -\frac{\Gamma}{\gamma_p} F_M(t, \boldsymbol{x}, \boldsymbol{p}) + \beta(\boldsymbol{x}, \boldsymbol{p}),$$
(1)

where $\boldsymbol{p}$ and $\boldsymbol{x}$ denote three-momentum and position of the meson, M, and $\boldsymbol{v} = \boldsymbol{p}/E_M(p)$ [m, $E_M(p) = \sqrt{m^2 + \boldsymbol{p}^2}$: meson mass and energy]. The total meson width, Γ, is assumed to be saturated by the coupling to quark-antiquark states, $M \leftrightharpoons q + \bar{q}$ and taken to be constant, with the factor $\gamma_p = E_M(p)/m$ accounting for Lorentz time dilation, see also Ref. [11]. Integrating over the fireball volume leads to the momentum-distribution function of the meson, f_M, and the pertinent transport equation

$$f_M(t, \boldsymbol{p}) = \int d^3x \, F_M(t, \boldsymbol{x}, \boldsymbol{p}),$$
$$\frac{\partial}{\partial t} f_M(t, \boldsymbol{p}) = -\frac{\Gamma}{\gamma_p} f_M(t, \boldsymbol{p}) + g(\boldsymbol{p}).$$
(2)

The drift term vanishes after integration over $\boldsymbol{x}$ because it is a total divergence: $\boldsymbol{v} \cdot \boldsymbol{\nabla} f_M(t, \boldsymbol{x}, \boldsymbol{p}) = \boldsymbol{\nabla} \cdot [\boldsymbol{v} f_M(t, \boldsymbol{x}, \boldsymbol{p})]$. The relation of the gain term, $g(\boldsymbol{p})$, to the underlying microscopic interaction is given by

$$g(\boldsymbol{p}) = \int d^3x \, \beta(\boldsymbol{x}, \boldsymbol{p}) = \int \frac{d^3p_1 d^3p_2}{(2\pi)^6} \int d^3x f_q(\boldsymbol{x}, \boldsymbol{p}_1)$$
$$\times f_{\bar{q}}(\boldsymbol{x}, \boldsymbol{p}_2) \sigma(s) \, v_{\text{rel}}(\boldsymbol{p}_1, \boldsymbol{p}_2) \delta^{(3)}(\boldsymbol{p} - \boldsymbol{p}_1 - \boldsymbol{p}_2) \quad (3)$$

with $\sigma(s)$ the cross section for the process $q + \bar{q} \rightarrow M$ at center-of-mass (c.m.) energy squared, $s = (p_1^{(4)} + p_2^{(4)})^2$, where $p_{1,2}^{(4)}$ are the four-momenta of quark and antiquark. The quark phase-space distribution functions are normalized as $N_{q,\bar{q}} = \int \frac{d^3x\, d^3p}{(2\pi)^3} f_{q,\bar{q}}(\boldsymbol{x}, \boldsymbol{p})$. Throughout this paper, quarks will be assumed to be zero-width quasiparticles with an effective mass m_q (that contains both thermal and bare contributions). The classical nature of the Boltzmann equation warrants the use of classical distribution functions for all the particles, and we assume zero chemical potentials for all quark species. The cross section is approximated by a relativistic Breit-Wigner form,

$$\sigma(s) = g_\sigma \frac{4\pi}{k^2} \frac{(\Gamma m)^2}{(s - m^2)^2 + (\Gamma m)^2}, \qquad (4)$$

where $g_\sigma = g_M/(g_q g_{\bar{q}})$ is a statistical weight given in terms of the spin (-color) degeneracy, $g_M(g_{q,\bar{q}})$, of the meson (anti-/quark), and k denotes the quark three-momentum in the c.m. frame. With $M \rightleftharpoons q + \bar{q}$ being the only channel, it follows that $\Gamma_{\text{in}} = \Gamma_{\text{out}} = \Gamma$. Detailed balance requires the same Γ in the loss term on the right-hand side of Eq. (1), thus ensuring the correct equilibrium limit with $\tau = 1/\Gamma$ the pertinent relaxation time. This formulation conserves four-momentum and applies to all resonances M with masses above the $q\bar{q}$ threshold, i.e., for a positive Q value,

$$Q = m - (m_q + m_{\bar{q}}) \gtrsim 0. \qquad (5)$$

If the $2 \rightarrow 1$ channel proceeds too far off-shell, i.e., $Q < 0$ and $\Gamma < |Q|$ (e.g., for pions), other processes need to be considered, e.g., $q + \bar{q} \rightarrow M + g$ (which, in principle, is possible in the present framework by implementing the respective cross sections). We note that the majority of the observed pions are believed to emanate from resonance decays (ρ, Δ, a_1, etc.); in addition, hydrodynamic calculations suggest that the elliptic flow in heavy-ion collisions at RHIC does not change much after hadronization [28]. We also note that in the absence of a confining interaction individual quarks and antiquarks remain a part of the heat bath. The equilibrium limit is readily recovered within our approach by imposing the stationarity condition,

$$\frac{\partial}{\partial t} f_M(t, \boldsymbol{p}) = 0. \qquad (6)$$

Then (2) is immediately solved by

$$f_M^{\text{eq}}(\boldsymbol{p}) = \frac{\gamma_p}{\Gamma} g(\boldsymbol{p}), \qquad (7)$$

which represents the large time limit of the Boltzmann equation and is the expression that comes closest to the conventional QCM approximation. For hadronization times less or comparable to the relaxation time, τ, the equilibrium limit will not be reached and an explicitly time-dependent solution is in order. We have verified numerically that Eq. (7) accurately recovers the standard thermal Boltzmann distribution for a meson M at temperature T, if the constraint of a positive Q value is satisfied (for negative Q the $2 \rightarrow 1$ channel is inoperative), as illustrated in Fig. 1 for the case of the ϕ meson: when using thermal quark input distributions with radial flow (blast-wave model), the computed equilibrium expression (7) is in excellent agreement with the same blast-wave expression
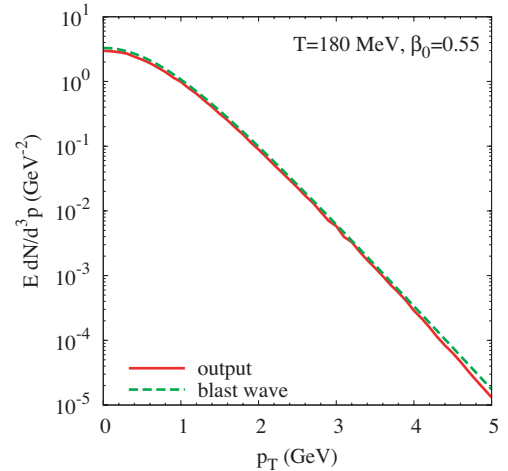

FIG. 1. (Color online) p_T spectra for ϕ mesons using the Boltzmann recombination equation in the equilibrium limit, Eq. (7), based on blast-wave input distributions for strange quarks (solid line), compared to ϕ spectra directly obtained from a blast-wave expression with the same fireball parameters (temperature $T = 180$ MeV, radial expansion surface velocity $\beta_0 = 0.55c$). The ϕ-meson resonance parameters are $m_\phi = 1.02$ GeV, $\Gamma_\phi = 50$ MeV, and the s-quark mass is $m_s = 0.45$ GeV.

(identical temperature and flow profile) directly applied at the meson level. This reiterates the close connection between equilibration and energy conservation in the approach of Ref. [12], providing a significant improvement of previous QCMs.

III. PARTONIC SPECTRUM

While the blast-wave model provides a convenient description of the thermal component of empirical hadron (and/or parton) spectra, the transition to the kinetic, and eventually hard-scattering, regime is more involved, especially with regard to phase-space correlations within QCMs, as discussed in the Introduction. In an attempt to generate realistic quark input distributions for meson formation processes in the vicinity of T_c, we here adopt a Fokker-Planck approach for test particles evolving in a thermally expanding QGP background. The latter is parameterized with guidance from hydrodynamic models for central and semicentral Au-Au collisions at RHIC, implementing empirical values (i.e., adjusted to experiment) for bulk matter properties such as total entropy, radial, and elliptic flow. The elliptic flow is parameterized in terms of a flow profile, whose direction at each transverse position is perpendicular to confocal elliptic isobars. Its magnitude is chosen to increase linearly in distance from the center with an average boundary value of $\beta_0 = 0.55c$ at the end of the mixed phase of the fireball evolution, i.e., at the hadronization time. The acceleration is adjusted so that the fireball at hadronization is approximately circular, with bulk $v_{2,q} \simeq 5.5\%$. This model has been employed before in the context of heavy-quark (HQ), i.e., charm and bottom spectra at RHIC [21], and good agreement with hydrodynamic simulations has been found [22] for the same HQ diffusion

coefficient. HQ observables, which at present are semileptonic single-electron decay spectra [29,30], exhibit an unexpectedly large suppression and elliptic flow that cannot be understood within perturbative QCD (pQCD), including both radiative and elastic scattering. The key microscopic ingredient in Ref. [21] are resonant heavy-light quark interactions mediated via effective (broad) D and B mesons in the QGP [31], inspired by the findings of thermal lattice QCD. In connection with a "conventional" coalescence afterburner [32] at T_c, the predictions for single-electron suppression and v_2 turned out to be in fair agreement with data [29,30]. In more recent work [25], the effective interactions have been replaced by in-medium T-matrices based on finite-temperature HQ potentials extracted from lattice QCD; these calculations not only confirmed the interaction strength generated by heavy-light resonances in an essentially parameter-free way but also identified prehadronic meson and diquark channels as the most relevant ones. This, in turn, provides a direct link between two main discoveries at RHIC, namely the strongly interacting nature of the sQGP and quark coalescence from a collective partonic source.

In the present article, we build on the above findings by extending the Fokker-Planck approach to strange (s) quarks. While its applicability criterion, $m_t \gg q \sim T$ ($m_t = \sqrt{m^2 + p_t^2}$: transverse mass, q: momentum transfer in a typical scattering), seems to be only marginally satisfied for momenta $p_t \lesssim 1$ GeV (at least in the early phases of the QGP evolution), we note that most of the fireball evolution occurs for temperatures close to T_c. At higher p_t (or m_t) one enters the kinetic regime where the Fokker-Planck treatment becomes reliable again. With these limits properly satisfied, one may hope that the Langevin simulations also accomplish a reasonable description of the low-p_t regime ($p_t \lesssim 1$ GeV) for strange quarks, including realistic space-momentum correlations, which is one of the main objectives in our work. The interaction strength of the strange- and charm-quark species remains to be specified. Here we take further guidance from phenomenology by requiring that the final quark $v_2(p_t)$ exhibits the characteristic saturation (or maximum) value of $\sim 7.5\%$. Our baseline interaction for the stochastic Langevin force is elastic pQCD scattering with a rather large value of $\alpha_s = 0.4$ (which can be thought of as containing radiative and/or parts of nonperturbative contributions). However, additional nonperturbative interactions are necessary to achieve a sufficiently large v_2. As in Refs. [21,31] we associate these with mesonic resonance states with an interaction strength controlled by the resonance width (with a larger width implying stronger coupling). For s quarks ($m_s = 0.45$ GeV) the "heavy-light" resonances require a width of $\Gamma_{s\bar{q}} \simeq 0.3$ GeV, and $\Gamma_{c\bar{q}} \simeq 0.6$ GeV for c quarks ($m_c = 1.5$ GeV), which is compatible with Refs. [21,31].[1] This hierarchy is qualitatively consistent with the general ex-

pectation that resonance/bound-state formation is suppressed with decreasing constituent mass (and also borne out of the microscopic T-matrix calculations for c and b quarks in Ref. [25]). Finally, we have to specify the initial quark distributions. For c quarks we use the initial spectra as constructed in Ref. [21], as to reproduce D-meson and semileptonic electron spectra in p-p and d-Au collisions. A similar procedure is adopted for strange quarks: we parametrize the quark spectra as a superposition of exponential and power-law spectra in a way that experimental kaon spectra in 200 GeV p-p collisions are properly reproduced (using δ-function fragmentation into kaons at half the parent-quark momentum; as usual in QCMs, the role of gluons is suppressed). In AA collisions, the exponential "soft" part is then scaled with the number of participants, N_{part}, and the power-law "hard" component with the number of collisions, N_{coll}, for a given centrality. With the interaction strengths and initial conditions fixed, the quark phase-space distribution in semi-/central Au-Au collisions are predicted from the Langevin simulations at the end of the QGP (mixed) phase without further adjustments and serve as an input for the meson formation processes as described in the previous section. The framework developed here, i.e., QGP evolution with resonance rescattering and recombination at T_c, will be referred to as a "resonance recombination model" (RRM).

The quark phase-space distributions resulting from the Langevin approach embody strong correlations between spatial and momentum variables. For example, quarks at high p_t tend to be located in the outer layers of the fireball with a preferential alignment of the momentum and position vector directions (i.e., the quark momentum tends to point "outward"). Likewise, the collective (radial and elliptic) flow, which implies a well-defined (hydro-like) correlation between the position of the fluid cell and its radial motion, imprints this correlation on the (partially) thermalized components of the Langevin-generated quark spectra. We recall again that the often used factorized implementation of the v_2 coefficient in coalescence models completely ignores these rather elementary dependencies.

The proper implementation of the differential phase-space information, carried by the quark distribution functions (which is essential for a realistic discussion of hadronic v_2-scaling properties), into the hadronization formalism requires a few technical remarks. Because thermalization in the longitudinal direction is somewhat controversial, we assume the quark distributions to be homogeneous in the spatial z-coordinate and flat in rapidity. This leaves four independent transverse variables for each particle, which we choose in azimuthal form, (p_t, ϕ_p, r_t, ϕ_r), corresponding to the distribution $dN_q/d^2p_t \, d^2r_t$. This 4D phase-space is then divided into finite bins (with a maximum value of $p_t^{\text{max}} \simeq 5$ GeV). For each simulated test quark, its final location and momentum is sorted into this grid. To warrant a (statistically) sufficiently smooth behavior of the computed meson observables, a sample of $\sim 10^8$ test particles is needed. Finally, an interpolation algorithm has been devised for converting the discretized distribution back into a continuous function, to be plugged into the hadronization formula. The algorithm recovers the periodicity properties of the two angular variables and converges to an

---

[1]We recall that according to Eq. (5) the only requirement on the quark and meson masses is that the latter are above the two-quark threshold; within this restriction variations in the mass and (positive) Q values have little effect on the recombination process. In fact, as we will see below, CQNS scaling emerges approximately independent of quark mass.

arbitrary sampled function in the limit of a large number of grid points. A suitable grid dimension corresponding to the above variables amounts to, e.g., (13, 96, 14, 12), where the large number of points in ϕ_p is dictated by the large sensitivity in the determination of the elliptic flow coefficient, $v_2(p_t)$.

We furthermore have to specify how to treat partons that escape the fireball prematurely, i.e., before the end of the QGP/mixed phase is reached. Clearly, these partons preferentially carry a high p_t, and, when exiting the fireball, could undergo a hadronization mechanism different from coalescence, such as fragmentation. Since our fireball is isotropic, the transition from the QGP to the vacuum is a sharp one and it would be unrealistic to coalesce the exiting quark with a thermal distribution at a temperature above T_c or at a time much later than the exit time (when the fireball has cooled down to T_c). We therefore decide to include only partons in our hadronization framework that remain inside the fireball throughout the entire QGP evolution. This leads to an underestimation of the high-momentum part of the hadronic spectra. A comprehensive calculation for quantitative comparison to experiment also at high p_t would require the treatment of the exiting partons (hadronized with either fragmentation or coalescence). Similarly, the hadronic v_2 we compute reflects only the partons within the QGP fireball at the end of its lifetime (which, however, do include nonthermal components from the Langevin simulation, in addition to the thermalized part of the spectrum).

The generated spectrum, which originally represents a probability distribution, requires a suitable normalization. Because the empirical light and strange hadron spectra are consistent with chemical equilibrium close to the expected phase boundary, we assume this to apply at the quark level as well, at the critical temperature $T_c = 180$ MeV of our fireball evolution. The fireball volume has been adjusted to match the total entropy of the fireball to the experimental hadronic final-state multiplicities at $T = 180$ MeV at given

collision centrality, e.g., $V_{FB} \simeq 1200$ fm^3 for semicentral Au-Au collisions (note that one fireball covers approximately 1.8 units in rapidity). For charm quarks we augment the chemical equilibrium number by a fugacity factor, $\gamma_c \simeq 5$ [33], to match their number to the expected hard production in primordial nucleon-nucleon collisions (binary collision scaling; in Ref. [12] $\gamma_c \simeq 8$ at $T_c = 170$ MeV leads to the same number of $c\bar{c}$ pairs in the fireball). We note, however, that the overall normalization has little impact on our main considerations of space-momentum correlations and v_2 systematics.

Let us finally specify the assumptions on the rapidity (y) distributions. As mentioned above, for both charm and strange quarks we employ a step function as

$$\frac{dN}{dy} = \frac{dN}{dy}\bigg|_{y=0} \theta\left(\frac{\Delta y}{2} - |y|\right), \qquad (8)$$

where the parameter Δy depends on the quark mass and has been adjusted to recover approximately the full-width-half-maximum of a thermal y spectrum (amounting to $\Delta y(s) = 1.3$ and $\Delta y(c) = 0.8$ in connection with the quark masses quoted above).

Figure 2 summarizes the results of the Langevin simulations for the p_t probability distributions (integrated over spatial coordinates) for c and s quarks, compared to (normalized) blast-wave spectra for $T = 180$ MeV, using the same flow field as in the Langevin simulation. The average surface-expansion velocity is $\langle\beta_0\rangle \simeq 0.48c$. At low p_t the spectra approach the equilibrium limit as to be expected because the background medium for the Langevin simulation is assumed to be fully equilibrated at all p_t, as in a hydrodynamic calculation, and the stochastic process has been realized as to guarantee the correct equilibrium limit including the adjustment of the (longitudinal) diffusion coefficient according to Einstein's fluctuation-dissipation relation [21]. As discussed above, the interaction strength has been chosen to recover the empirically observed maximum elliptic flow of $v_{2\cdot q}^{max} \simeq 7$–8%.
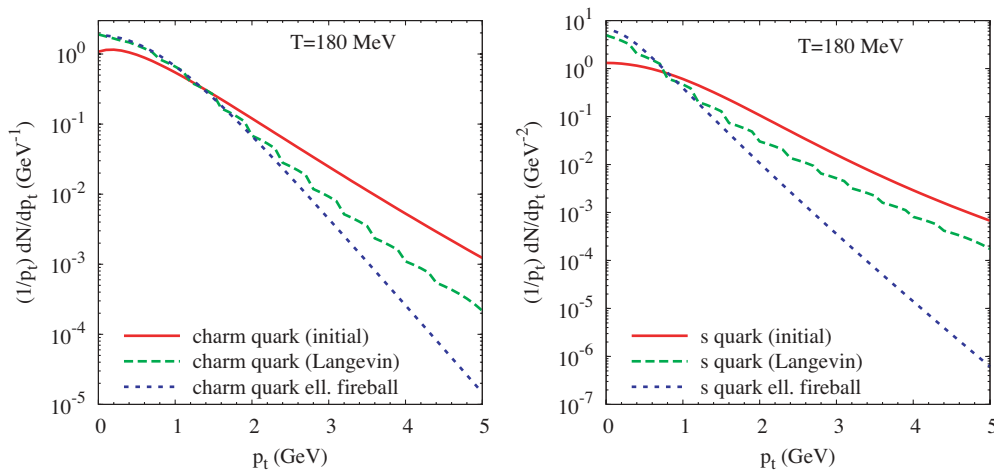

FIG. 2. (Color online) Quark p_t distributions resulting from relativistic Langevin simulations of an expanding elliptic QGP fireball at the end of a QGP (mixed) phase at a temperature of $T = 180$ MeV and average radial surface expansion velocity, $\langle\beta_0\rangle \simeq 0.48c$. The numerically computed spectra (long-dashed lines) are compared to the initial spectra (solid lines) and to a blast-wave parametrization for particles with the same mass and the same fireball conditions ($T = 180$ MeV and the same flow field as used for the background medium in the Langevin simulation; short-dashed lines). Left and right panels correspond to charm ($m_c = 1.5$ GeV) and strange ($m_s = 0.45$ GeV) quarks, respectively.
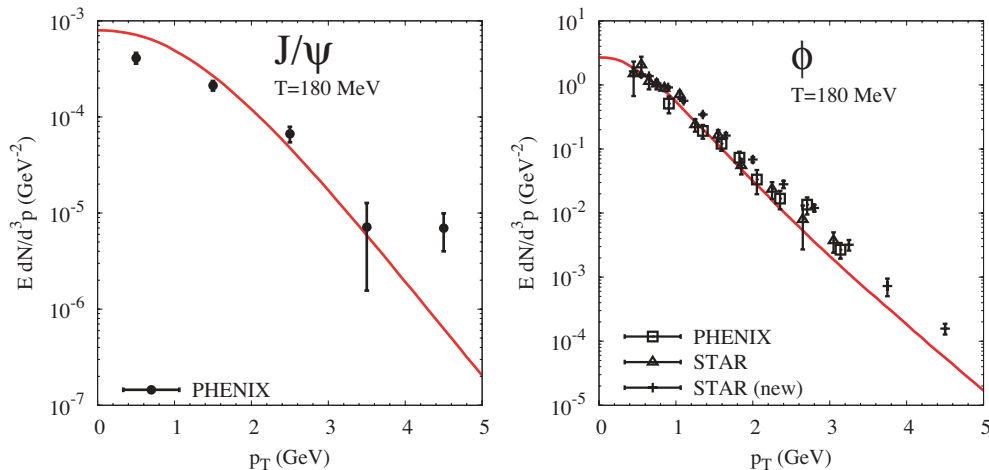
FIG. 3. (Color online) Meson p_T spectra from quark-antiquark coalescence in central $\sqrt{s_{NN}} = 200$ GeV Au-Au collisions computed within the resonance recombination model for J/ψ (left panel) and ϕ (right panel); experimental data are from Refs. [36] and [37–39], respectively.

Note, however, that the assumption of a fully thermalized background medium implies rather large v_2 values at high p_t, while the phase-space density of thermal partons is rather small. A full treatment of this problem would require to solve a self-consistency problem, where the parton spectra in the background fireball evolution also exhibit a saturation of the elliptic flow, $v_2(p_t)$. This is beyond the scope of the present article.

IV. MESON p_T SPECTRA AND v_2 SYSTEMATICS

We now combine the ingredients of our resonance recombination model (RRM) by implementing the quark spectra computed from Langevin simulations in Sec. III with the Boltzmann-based hadronization formalism of Sec. II, evaluated in the stationary (equilibrium) limit according to Eq. (7). The key issue we address is how the properties of the input (nonobservable) quark spectra reflect themselves in the (observable) meson spectra, in particular whether the space-momentum correlations generated in the Langevin simulations can be consistent with the empirically observed CQNS, which, in turn, opens a window on the quark spectra at hadronization.

The masses and widths of hadrons in the recombination process remain to be specified. In line with our restriction to mesons located above the quark-antiquark threshold (due to the limitation to $2 \to 1$ processes) we consider s-$\bar{s}$, c-$\bar{c}$ coalescence with resonance masses corresponding to the vacuum values for ϕ (1.02 GeV) and J/ψ (3.1 GeV) mesons; in connection with the quark masses as given above this implies similar Q values of 0.1–0.12 GeV. The (total) meson widths are chosen of comparable magnitude, i.e., $\Gamma_\phi = 0.05$ GeV and $\Gamma_{J/\psi} = 0.1$ GeV. As elaborated in Ref. [12], the numerical results, especially for the meson v_2, are rather insensitive to variations in the meson width as long as Q is positive and substantially smaller (not smaller) than the resonance mass (width).

In Fig. 3 we display our RRM results for p_T spectra of J/ψ and ϕ mesons, including available RHIC data. Overall, the spectra largely agree with those computed in our previous work (Fig. 1 in Ref. [12]), where the input spectra were solely based on a blast-wave parametrization. This is not surprising, because the quark spectra employed in the present work show a rather large degree of thermalization, up to momenta of $p_t = 1.5$–2 GeV for strange and charm quarks, cf. Fig. 2. Consequently, the ϕ-meson spectra shown here are somewhat harder than in Ref. [12] beyond $p_T \simeq 3$ GeV due to the presence of the kinetic (hard) components in the quark spectra resulting from the Langevin evolution. The computed spectra for the J/ψ are quite reminiscent to earlier blast-wave based results [32,34,35]. Note, however, that in Ref. [35] the recombination (blast wave) contribution only amounts to about 50% of the total J/ψ yield, significantly less than in the present article (this is sensitive to the total open-charm cross section, which is not very well determined yet).

The RRM results for the meson $v_2(p_T)$ are summarized in Fig. 4 (solid lines) and compared to the underlying quark v_2 scaled to meson variables in the conventional (empirical) way as $v_2^{\text{scaled}}(p_T) \equiv 2v_{2,q}(p_T/2)$. We find that for both the J/ψ and ϕ the agreement is rather impressive, within a few percent of relative deviation. The wiggles at the quark level are, to a large extent, driven by the finite grid sampling due to a step width of 400 MeV (the statistical error inherent to the Langevin simulation is smaller than that, using 10^8 test particles). The convolution of two quark distributions results in much smoother curves at the meson level (due to the fitting procedure of the quark input). We are thus able to approximately recover CQNS in a microscopic calculation with the full information on space-momentum correlations, characteristic for hydrodynamic expansion at low p_t and a kinetic regime at higher p_t.

Another potential source for scaling violations are flavor (or mass) dependencies at the quark level (rather than in the coalescence process). In Fig. 5 we compare the elliptic flow of different quarks (left panel) and mesons (right panel) with each other. The left panel confirms that the c-quark v_2 deviates
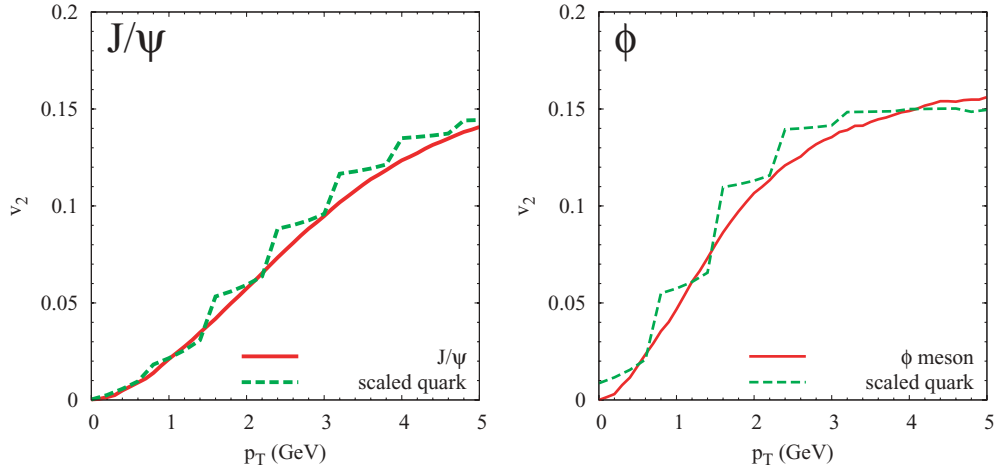
FIG. 4. (Color online) Scaled quark v_2^{scaled} (dashed lines) and meson $v_{2,M}$ (solid lines) coefficients as a function of meson p_T for $J/\Psi(Q = 0.1$ GeV, $\Gamma = 0.1$ GeV; left panel) and $\phi(Q = 0.12$ GeV, $\Gamma = 0.05$ GeV; right panel) mesons.

significantly (up to $\sim$20% at low p_t) from the strange-quark v_2. At high p_t, the strange-quark v_2 is a bit high, which, in principle, could be readjusted by a somewhat reduced strength of the resonance interactions in the Langevin simulations. At the meson level, the differences are similar. We have verified that comparable deviations persist when reducing the strange quark v_2.

Finally, we address the question of CQNS with respect to transverse kinetic energy, $K_T = m_T - m$, rather than transverse momentum, p_T. Such a scaling has recently been highlighted by the PHENIX [19] and STAR Collaborations [20] and seems to be very well satisfied by all available RHIC data, in centrality, collision energy and collision systems, after a geometric correction for the nuclear overlap. K_T scaling has also been found to result from certain classes of hydrodynamic solutions [40], and therefore been argued to reflect a collectively expanding thermalized system of partons [41]. From the point of view of quark coalescence,

the problem of reconciling quark distribution functions with space-momentum correlations (as implied by hydrodynamic expansion) with CQNS persists. In Fig. 6 we display the RRM results for $v_{2,q}$ and $v_{2,M}$ for the two different flavors as a function of $K_{t,T}$. We find that the quark input distributions from the QGP Langevin simulations indeed share a rather universal behavior up to $K_t \simeq 3$ GeV, encompassing both the quasiequilibrium regime at low energies and the kinetic regime at intermediate energies characterized by a leveling off at $K_t \gtrsim 1$ GeV, cf. left panel of Fig. 6. We recall that the only adjusted input to this result is the common maximum value of the individual quark elliptic flow at about 7–8% (as suggested by the empirical CQNS deduced from experiment), controlled by the nonperturbative interaction strength in the stochastic Langevin force (again, a fine tuning for the s quark would improve the agreement at higher K_t). The approximate universality at the quark level is nicely preserved at the meson level as a result of our Boltzmann-based recombination
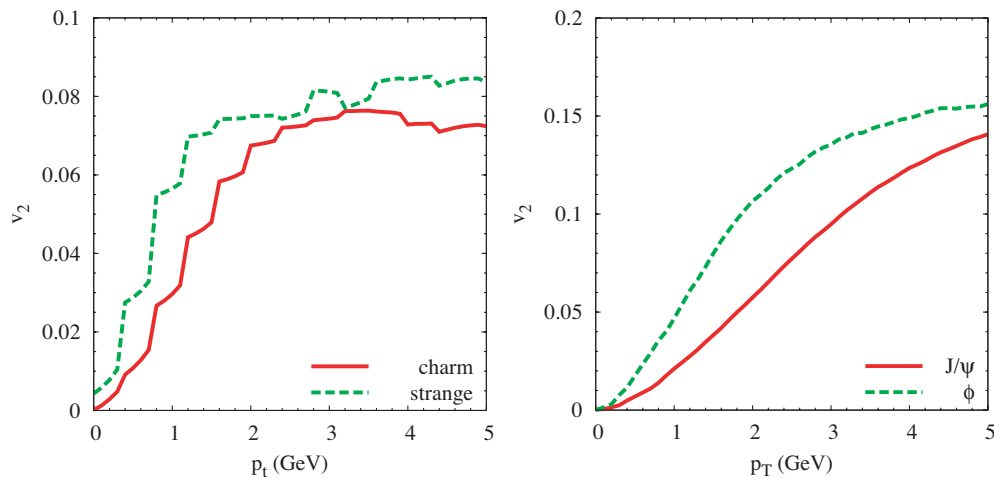

FIG. 5. (Color online) Elliptic flow coefficient, v_2, as a function of transverse momentum for c and s quarks (left panel), as well as J/ψ and ϕ mesons resulting from quark recombination (right panel), in semicentral $\sqrt{s_{NN}} = 200$ GeV Au-Au collisions.
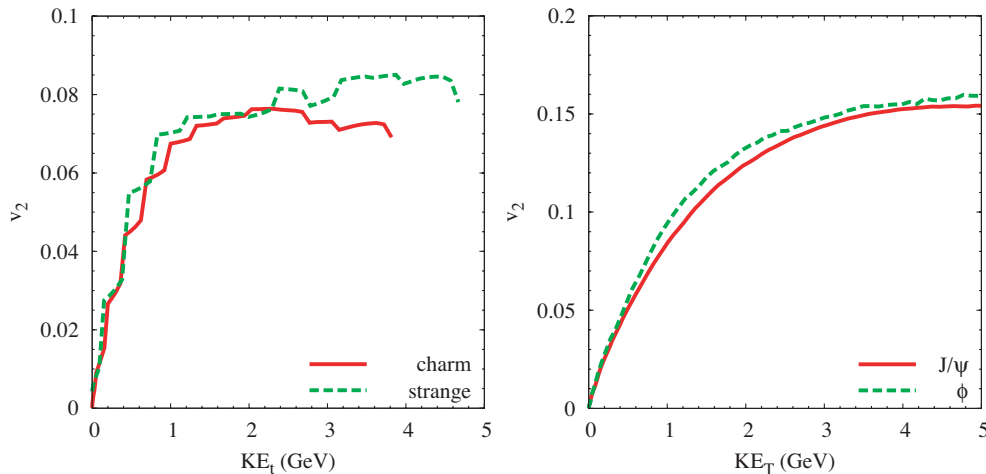
FIG. 6. (Color online) Elliptic flow coefficient, v_2, as a function of transverse kinetic energy, $K_{t,T}$, for strange and charm quarks (left panel), as well as for ϕ and J/ψ mesons (right panel).

formalism; see right panel of Fig. 6. This is a quite remarkable result in view of the underlying space-momentum correlations in our approach, which has not been achieved before in this form.

V. CONCLUSIONS

In the present article we have extended our previously formulated quark coalescence formalism, using resonance interactions within a Boltzmann equation, by implementing microscopic quark phase-space distributions generated via Langevin simulations of an expanding thermal QGP fireball for Au-Au collisions at RHIC. In this way we could combine the merits of our recombination approach (energy conservation and a proper equilibrium limit) with those of realistic quark distributions, which in particular encode the transition from a thermal regime at low p_t to a kinetic one at intermediate p_t. The latter feature is especially important as it produces the leveling-off of the elliptic flow, a key feature of observed hadron spectra and a crucial prerequisite to test any kind of quark scaling behavior. The (constituent) quark-mass and meson parameters were fixed at rather standard values, and we have constrained ourselves to mesons that are reliably calculable in our $2 \rightarrow 1$ recombination setup (i.e., for positive Q values). The only real adjustment concerned the interaction strength in the Langevin process, as to reproduce the empirical maximum value for the quark v_2 (with the QGP fireball parameters tuned to empirical values of radial and elliptic flow, as in earlier applications to, e.g., heavy-quark observables). These interactions have been modeled via (meson) resonances in the QGP, which we identified with the states formed in the coalescence process at T_c, leading to the notion of an RRM. Because the Fokker-Planck approach as an expansion of the Boltzmann equation is strictly valid for sufficiently massive and/or high-momentum particles, we restricted ourselves to "heavy" flavors, i.e., charm and strange quarks. At low p_t, the latter are at the borderline of applicability of a Fokker-Planck framework.

Our main finding is that within this rather generic set-up, largely based on first principles augmented by a concrete realization of the strongly interacting QGP, the constituent quark scaling of the meson elliptic flow emerges rather naturally, *including* space-momentum correlations characteristic for a collectively expanding source. The scaling holds for individual mesons but appears to be rather universal in quark and meson flavor (mass), especially when applied in (transverse) kinetic energy rather than momentum, which is in line with recent experimental findings. By overcoming some of the limitations of previous (more schematic) coalescence models, and by achieving the first robust implementation of realistic (microscopically computed) phase-space distribution functions of quarks, our formalism could provide a useful tool to better understand systematics of RHIC data, most notably the interplay of a thermal and kinetic regime in connection with phase-space properties of the partonic fireball as viewed through the hadronization process.

Clearly, a formidable list of open issues persists, including the extension to light quarks, the role of gluons and of deeply bound hadronic states (possibly requiring additional formation processes), more realistic spectral functions of mesons and quarks and their interactions (both around T_c and above), a self-consistent treatment of thermal and kinetic components (possibly requiring full parton transport), a systematic classification of viable parton phase-space distributions, hadronic reinteractions, etc. Progress has already been made on a number of these aspects, but a comprehensive approach remains a challenging task.

[1] K. P. Das and R. C. Hwa, Phys. Lett. **B68**, 459 (1977) [Erratum-*ibid.* **B73**, 503 (1978)].

[2] E. Braaten, Y. Jia, and T. Mehen, Phys. Rev. Lett. **89**, 122002 (2002).

[3] R. Rapp and E. V. Shuryak, Phys. Rev. D **67**, 074036 (2003).

[4] T. S. Biro, P. Levai, and J. Zimanyi, Phys. Lett. **B347**, 6 (1995).

[5] R. C. Hwa and C. B. Yang, Phys. Rev. C **67**, 034902 (2003).

[6] V. Greco, C. M. Ko, and P. Levai, Phys. Rev. C **68**, 034904 (2003).

[7] R. J. Fries, B. Müller, C. Nonaka, and S. A. Bass, Phys. Rev. C **68**, 044902 (2003).

[8] D. Molnar and S. A. Voloshin, Phys. Rev. Lett. **91**, 092301 (2003).

[9] Z.-W. Lin, C. M. Ko, B.-A. Li, B. Zhang, and S. Pal, Phys. Rev. C **72**, 064901 (2005).

[10] J. Zimanyi, P. Levai, and T. S. Biro, J. Phys. G **31**, 711 (2005).

[11] H. Miao, C. Gao, and P. Zhuang, Phys. Rev. C **76**, 014907 (2007).

[12] L. Ravagli and R. Rapp, Phys. Lett. **B655**, 126 (2007).

[13] A. Ayala, M. Martinez, G. Paic, and G. T. Sanchez, Phys. Rev. C **77**, 044901 (2008).

[14] W. Cassing and E. L. Bratkovskaya, Phys. Rev. C **78**, 034919 (2008).

[15] R. J. Fries, V. Greco, and P. Sorensen, Annu. Rev. Nucl. Part. Sci. **58**, 177 (2008).

[16] S. Pratt and S. Pal, Nucl. Phys. **A749**, 268 (2005).

[17] D. Molnar, arXiv:nucl-th/0408044.

[18] V. Greco and C. M. Ko, arXiv:nucl-th/0505061.

[19] A. Adare *et al.* (PHENIX Collaboration), Phys. Rev. Lett. **98**, 162301 (2007).

[20] B. I. Abelev *et al.* (STAR Collaboration), Phys. Rev. C **75**, 054906 (2007).

[21] H. van Hees, V. Greco, and R. Rapp, Phys. Rev. C **73**, 034913 (2006).

[22] G. D. Moore and D. Teaney, Phys. Rev. C **71**, 064904 (2005).

[23] E. V. Shuryak and I. Zahed, Phys. Rev. D **70**, 054507 (2004).

[24] M. Mannarelli and R. Rapp, Phys. Rev. C **72**, 064905 (2005).

[25] H. van Hees, M. Mannarelli, V. Greco, and R. Rapp, Phys. Rev. Lett. **100**, 192301 (2008).

[26] F. Karsch and E. Laermann, in *Quark-Gluon Plasma*, edited by R. C. Hwa and X. N. Wang (World Scientific, Singapore, 2004), Vol. 3, p. 1.

[27] M. Asakawa and T. Hatsuda, Nucl. Phys. **A721**, 869 (2003).

[28] P. F. Kolb and U. W. Heinz, in *Quark-Gluon Plasma*, edited by R. C. Hwa and X. N. Wang (World Scientific, Singapore, 2004), Vol. 3, p. 634.

[29] A. Adare *et al.* (PHENIX Collaboration), Phys. Rev. Lett. **98**, 172301 (2007).

[30] B. I. Abelev *et al.* (STAR Collaboration), Phys. Rev. Lett. **98**, 192301 (2007).

[31] H. van Hees and R. Rapp, Phys. Rev. C **71**, 034907 (2005).

[32] V. Greco, C. M. Ko, and R. Rapp, Phys. Lett. **B595**, 202 (2004).

[33] L. Grandchamp, R. Rapp, and G. E. Brown, Phys. Rev. Lett. **92**, 212301 (2004).

[34] A. Andronic, P. Braun-Munzinger, K. Redlich, and J. Stachel, Nucl. Phys. **A789**, 334 (2007).

[35] X. Zhao and R. Rapp, Phys. Lett. **B664**, 253 (2008).

[36] A. Adare *et al.* (PHENIX Collaboration), Phys. Rev. Lett. **98**, 232301 (2007).

[37] S. S. Adler *et al.* (PHENIX Collaboration), Phys. Rev. C **72**, 014903 (2005).

[38] J. Adams *et al.* (STAR Collaboration), Phys. Lett. **B612**, 181 (2005).

[39] B. I. Abelev *et al.* (STAR Collaboration), Phys. Rev. Lett. **99**, 112301 (2007).

[40] M. Csanad *et al.*, Eur. Phys. J. A **38**, 363 (2008).

[41] R. A. Lacey and A. Taranenko, PoS C **FRNC2006**, 021 (2006).

[42] T. Hahn, Comput. Phys. Commun. **168**, 78 (2005).